

HIGHLY LOADED CERAMIC PARTICLE REINFORCED METAL: ROLE OF PARTICLE FRACTURE

Aude Hauert*, Andreas Rossoll*, Andreas Mortensen*

*Ecole Polytechnique Fédérale de Lausanne, Laboratory for Mechanical Metallurgy,
EPFL Station 12, Lausanne CH-1015, Switzerland.

Keywords: *metal matrix composite, particle fracture, aluminium, alumina, mean-field analysis, tensile ductility.*

Abstract

We draw a parallel between particle and fibre reinforced composites to explore parameters governing the failure of highly loaded ceramic particle reinforced aluminium alloys. Particle strength is supposed to follow a Weibull distribution. Final fracture may occur by one of two modes: (i) the onset of tensile instability or (ii) catastrophic failure, i.e., unstable propagation of particle breaks into neighbouring particles. We show that if particle properties match documented values for ceramic fibres, the composites encounter almost no particle damage. With lower particle strength, the present analysis can mimic in fairly realistic fashion the behaviour of particle reinforced metal matrix composites, showing a transition from failure by tensile instability to catastrophic fracture with an increase of matrix strength.

1 Introduction

Ceramic particle reinforced metals are attractive from several standpoints but often show poor ductility compared with unreinforced engineering metals and alloys. At first sight, this seems intuitively obvious: adding a (brittle) ceramic to a (ductile) metal should make the latter more brittle. Looking at the question in more depth, however, the question is far less trivial, first because the underlying mechanics are complicated, and secondly because, as is well known, when small, ceramics can be very strong.

Significant strides in our understanding of this complicated problem have been accomplished over the past decade. Reliable and realistic mechanical models for the deformation of metal/ceramic composites into the non-linear regime now exist in both main model classes, comprising (i) mean-field

models, which propose analytical expressions that capture relatively well average phase stress and strain states in two-phase composites, and (ii) numerical models, which capture with precision microscopic distributions of stress and strain within complex three-dimensional multi-inclusion unit cells (e.g., [1-5]).

The nature and evolution of internal damage within these materials have been a particular focus of interest. It is well known that there are three modes of internal damage, namely particle fracture, matrix voiding, and interfacial debonding [5, 6]. All three have also been treated in micromechanical modelling of particle reinforced metal deformation [7-11]. Of these three damage modes, interfacial debonding is less interesting because it signals a defective material. The other two are, on the other hand, critical: matrix voiding because it is exacerbated by the particles, and particle cracking because it is mainly by this mechanism that the embrittling influence of the ceramic particles is manifest.

Research at EPFL on the deformation and fracture of particle reinforced metals has placed focus on highly loaded ceramic particle reinforced aluminium composites produced in the laboratory using pressure-infiltration; Fig. 1 gives an example of their microstructure. In these composites, all particles are tightly packed; hence particle clustering, known to be an important complicating factor in the fracture of particle reinforced metals [2, 12-14], need not be considered. Also, since these materials are produced by pressure infiltration, a wide array of microstructurally tailored composites can be made, featuring strong interfaces, particles of controlled nature and size, and a uniform, tailored and pore-free matrix. Reports of the processing, main features and tensile behaviour of these model composite materials can be found in [15-17].

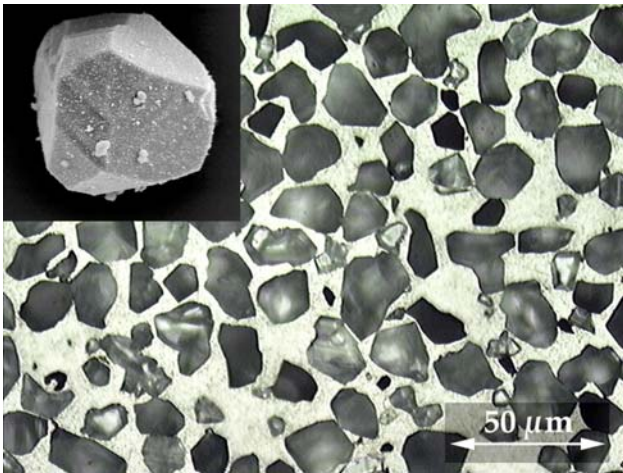


Fig. 1. Typical microstructure of high volume fraction Sumicorundum™ particle reinforced aluminium composite produced by gas pressure-infiltration.

This article builds on two findings from this research program to draw a parallel between these composites and ceramic fibre reinforced metals.

The first finding is the clarity with which intrinsic properties of the ceramic particles are seen in the mechanical behaviour of these composites: better particles make far better composites. The difference between comminuted Bayer-type alumina and vapour-grown Sumicorundum™ alumina particles is eloquent: the latter are visibly far superior, yielding composites having combinations of strength and toughness that match those of engineering aluminium alloys; see Refs. [18, 19].

The second finding that suggests a parallel with fibre reinforced metals is that these composites fracture, in tension, in one of two modes, Fig. 2(a). The first failure mode, found with ductile matrices (pure aluminium notably), is by tensile instability, as manifest by a smooth maximum on the engineering stress-strain curve. With stronger matrices and smaller particles, on the other hand, failure tends to be abrupt, denoting essentially brittle behaviour. In both cases, Fig. 2(b), tensile failure is preceded by extensive build-up of internal damage, which clearly governs the tensile failure of the composites and, hence, strongly influences their tensile ductility.

These two observations, taken together, suggest a parallel between these materials and relatively similar composites of ceramic fibre reinforced metal. In continuous fibre reinforced metals too, the reinforcement strength matters immensely. Also, with tightly packed brittle fibres as with tightly packed particles, tensile failure is seen to occur in one of two modes, either featuring a

gradual build-up of uncorrelated damage resulting in a tensile curve with a relatively smooth maximum, or alternatively by abrupt failure as a result of a localized propagation of internal damage [20-22].

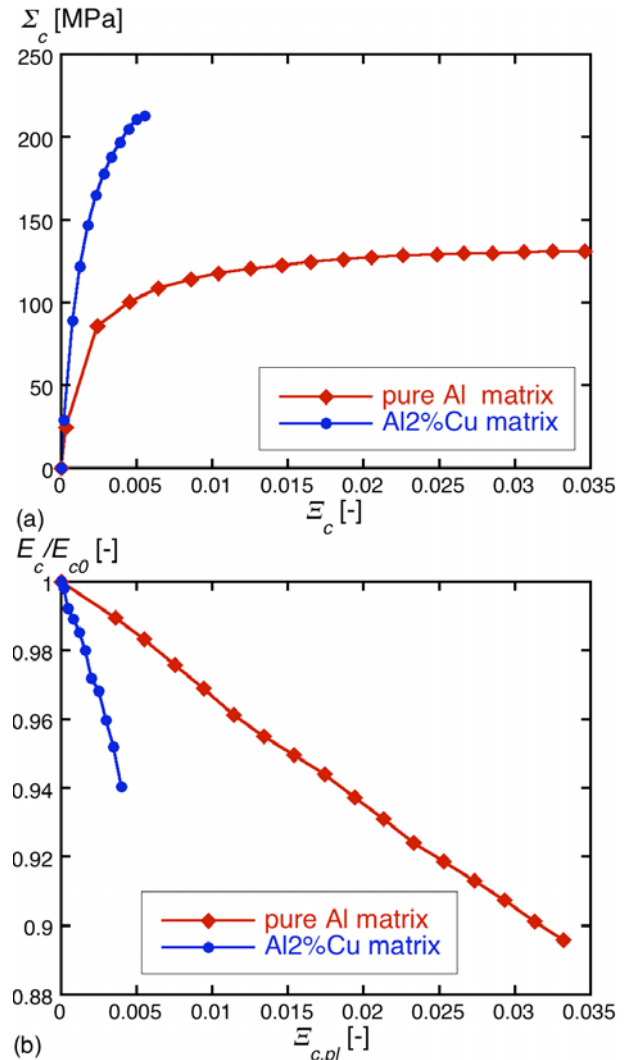


Fig. 2. Pure aluminium and Al-2%Cu alloy reinforced with angular 35 micron alumina particles. (a) Typical true stress-strain curves, and (b) the evolution of Young's modulus (normalized by its initial value) as a function of plastic strain.

We build here on this parallel to probe the limits of what can be achieved in the reinforcement of metals if very strong ceramic particles are used. We use to this end a mean-field analysis method that has recently been proposed by simplification of current micromechanical models for the deformation of non-linear composites [23]. As will be seen, even though the calculations are strongly simplified, clear conclusions emerge concerning the microstructural design and the potential of particle reinforced metals, particularly at high ceramic volume fractions.

2 The Analogy with Fibre Reinforced Metals

Consider a composite of a ductile metal reinforced with very strong ceramic particles. We assume that the material damages and fails under tension by only one damage mechanism, namely fracture of the particles: matrix voiding is thus ignored altogether here.

A first difficulty is to define what exactly constitutes a “very strong” ceramic particle: to this end, we use a simple argument, namely that what has been achieved in strong ceramic fibres must be attainable also in ceramic particles of comparable size. Table 1 gives statistical strength data from the literature for four metal-compatible high-strength fibres. As a reference volume V_0 in this table, we have taken that of a spherical particle having a diameter of 25 μm .

Table 1. Weibull parameters for different (fibre) reinforcements.

	$V_0 [\mu\text{m}^3]$	$\sigma_0 [\text{GPa}]$	m
Nextel™ Al ₂ O ₃ [24]	8181	5.4	12
Alltex™ Al ₂ O ₃ [25]	8181	9.6	4
Carbon [26]	8181	8.3	4.5
SiO ₂ [27]	8181	9	14

A realistic treatment of tensile failure in the composites should address both observed failure modes noted above, i.e., brittle or ductile fracture. We do so again by analogy with unidirectional fibre reinforced composites, by considering two fracture modes that represent extremes in behaviour of these materials under longitudinal loading, namely their well-known local and global load sharing fracture modes [20, 21].

Failure by global load sharing occurs by the progressive uncorrelated accumulation of damage within the composite; this causes a progressive decrease in the composite flow stress, causing it to peak smoothly. We assume that failure occurs when Considere’s criterion is fulfilled, i.e., when the rate of work hardening equals the flow stress. In doing so we neglect the influence of density changes caused by the opening of cracked particles in the composite on the onset of tensile instability; in the present composites this does not make a significant difference; see [28].

Abrupt failure, on the other hand, signals that internal damage can propagate within the material to “cut” the composite in half before the onset of tensile instability. The inhomogeneous coalescence of damage in heterogeneous materials is an

exceedingly complex problem. To tackle this quantitatively we again draw a parallel with fibre reinforced composites, where this problem is relatively well understood. We thus adapt a well-known model for fibre composite failure by “local load sharing”, to describe in simple terms the statistical propagation of particle breaks from one particle to its neighbours, with a goal of estimating when the process becomes catastrophic.

3 Simplified Analysis

Consider a simple two-phase material of a ductile power-law metal reinforced with homogeneously distributed brittle spherical ceramic particles that break statistically according to a classical two-parameter Weibull law. The particles are strongly bonded to the metal, and the metal does not damage by voiding or otherwise. Hence, particle fracture is the only active internal damage mechanism that we consider here.

The flow curve of the undamaged composite material is modelled using the linear Mori-Tanaka mean-field scheme extended for a non-linear matrix flow stress by means of the variational estimate of Ponte-Castañeda and Suquet, simplified as described in [23] for uniaxial deformation by assuming an incompressible matrix and a rigid reinforcement. In what follows, we will refer to this model as the VE-MT model.

Under uniaxial tensile loading, the composite undergoes progressive damage by particle cracking. Many approaches and expressions have been proposed to model the deformation of a composite containing a non-linear matrix and part-cracked, part-intact ceramic particles. For example, in mean-field models cracked particles have been assimilated to small matrix cracks [7, 29] or to internal voids [30]. These assumptions are questionable because they overestimate the reduction in load-bearing capacity caused by broken particles; also, they yield rather unwieldy expressions for the damaged composite flow stress (because it is described as a three-phase composite, one of the reinforcements also often being anisotropic). We make here a different assumption, which is described and justified in detail elsewhere: we assume that deformation around a cracked spherical particle in a far more compliant matrix is adequately simulated by replacing the cracked particles with an equal amount of matrix phase [31, 32]. With this assumption, a damaging composite becomes one that simply sees a progressive reduction in its volume

fraction ceramic, all mechanical expressions remaining those of a two-phase material.

3.1 Computing the Stress-Strain Curve of the Damaging Composite

The modelled composites are made of aluminium or its alloy reinforced with particles, with a volume fraction of reinforcement (V_r) of 50%. In what follows, indices c , m , $r1$ and $r2$ refer to the composite, matrix, intact and broken reinforcements, respectively.

The matrix is assumed to harden according to an isotropic Hollomon power-law:

$$\sigma_{m,eq} = c \cdot \varepsilon_{m,eq}^n \quad (1)$$

where $\sigma_{m,eq}$ is the matrix equivalent stress, $\varepsilon_{m,eq}$ the matrix equivalent plastic strain, c the strength coefficient and n the hardening exponent. The matrix is an Al-4.5%Cu alloy with $c = 628$ MPa and $n = 0.17$. These *in-situ* matrix constitutive law parameters result from “back-calculation” using the VE-MT model in conjunction with data from tensile tests for composites reinforced with 50 to 60% of 25 μm polygonal alumina particles, as described elsewhere [33].

The strength of the reinforcing particles is assumed to follow a two-parameter Weibull distribution:

$$f_b = 1 - \exp\left[-\frac{V}{V_0} \cdot \left(\frac{\sigma_r}{\sigma_0}\right)^m\right] \quad (2)$$

with f_b the fraction of broken particles, V_0 the reference volume, σ_0 the stress at which the fracture probability equals 63% for a particle of volume V_0 , m the Weibull modulus, σ_r the longitudinal tensile stress acting on the particles, and V the volume of a single particle.

As the Weibull parameters of ceramic particles are not directly assessable from experiment, we use measured Weibull characteristics of ceramic fibres reported in the literature, Table 1 [24-27].

During tensile deformation, the composite is assumed to accumulate damage by particle cracking. By definition of the present mean-field model, all intact particles are subjected to the same stress. Particle cracking is thus governed by the average particle stress along the tensile direction, $\langle \sigma_{r1}^1 \rangle$. Thus, knowing the Weibull parameters of the reinforcements, $\langle \sigma_{r1}^1 \rangle$ is known for a given fraction of broken particles f_b :

$$\langle \sigma_{r1}^1 \rangle = \sigma_0 \cdot \left[\frac{V_0}{V} \cdot \ln\left(\frac{1}{1-f_b}\right) \right]^{\frac{1}{m}} \quad (3)$$

where:

$$f_b = \frac{V_{r2}}{V_{r1} + V_{r2}} \quad (4)$$

with V_{r2} the volume fraction of damaged particles and V_{r1} the volume fraction of intact particles.

For this known fraction of broken particles and a given initial volume fraction of particles, if we ignore the complications induced by local matrix unloading upon particle fracture (this assumption is discussed in more detail in [32]), the stress carried by the composite along the tensile direction Σ_c^1 is related to $\langle \sigma_{r1}^1 \rangle$ via:

$$\Sigma_c^1 = V_{r1} \cdot \langle \sigma_{r1}^1 \rangle + (V_m + V_{r2}) \cdot \langle \sigma_m^1 \rangle \quad (5)$$

with $\langle \sigma_m^1 \rangle$ the average stress borne by the matrix along the tensile direction calculated by means of the “modified” secant matrix stress concentration factor, B_{ms} , defined in Eq. 6 for the plastic regime (matrix elastic deformation is neglected here):

$$\langle \sigma_m^1 \rangle = B_{ms} \cdot \Sigma_c^1 \quad (6)$$

The Mori-Tanaka model simplified for an incompressible matrix and rigid intact particles gives the following simple expression for B_{ms} :

$$B_{ms} = \frac{2 + V_{r1}}{2 + 3V_{r1}} \quad (7)$$

The axial stress borne by the composite can thus be calculated using Eqs. 3 to 7 knowing V_{r1} and V_{r2} . The corresponding composite strain can be calculated as follows.

With the assumptions of the VE-MT model, for a constant fraction of ceramic particles, the composite behaves as a power-law von Mises plastic material having the same exponent n as the matrix:

$$\Sigma_{c,eq} = C \cdot \Xi_{c,eq}^n \quad (8)$$

with $\Sigma_{c,eq}$ and $\Xi_{c,eq}$ the composite equivalent stress and strain, respectively. Since uniaxial tensile loading is considered, these equivalent values are equal to the stress and strain in the loading direction.

Finally, the ratio C/c of the composite strength coefficient C over the matrix strength coefficient c can be obtained as outlined in [23]:

$$\frac{C}{c} = \frac{\left(\frac{3}{2}V_{r1} + 1\right)^{\frac{n+1}{2}}}{(1-V_{r1})^n} \quad (9)$$

The strain in the composite with a given amount of broken particles is thus given by Eqs. 8 and 9. Varying the fraction of broken reinforcements, the entire stress-strain curve of the composite can then be simulated.

3.2 Fracture Simulated by the Onset of Tensile Instability

The onset of tensile instability is met when the Considere criterion (Eq. 10) is fulfilled.

$$\Sigma_c^1 = \frac{d\Sigma_c^1}{d\varepsilon_c^1} \quad (10)$$

Both terms in this equation are calculated directly from the model described in Section 3.1.

In the present mean-field calculation, the key underlying assumption is that damage accumulation in the composite is governed by the average stress borne by the particles. Now, it has been shown in recent finite-element simulations of large three-dimensional cells of ductile metallic materials containing large numbers of randomly distributed hard ceramic particles that the stress within the particles is highly heterogeneous, both inside the particles and also from particle to particle [4, 13, 34-36]. This can cause a reduction in composite strength for a statistical distribution of particle strengths since, for a given average composite and hence particle stress, local stress peaks within the particles may cause them to fracture prematurely.

To account for the influence of this effect, we assume that, keeping all other elements of the analysis the same, the particle stress is distributed around its average $\langle \sigma_{r1}^1 \rangle$, either with a rectangular or a triangular distribution. To simplify the subsequent derivation, we assume that particle fracture is governed by the low-stress expansion of the two-parameter Weibull law; i.e., we simplify Eq. 2 as:

$$f_b \cong \frac{V}{V_0} \cdot \left(\frac{\sigma_r}{\sigma_0} \right)^m \quad (11)$$

This approximation is valid for small amounts of broken particles, i.e., less than 10% for Weibull parameters such as those presented in Table 1.

For a given particle stress distribution and $\langle \sigma_{r1}^1 \rangle$ the average stress acting on the intact particles, the particle fracture probability, i.e., the fraction of broken particles, is:

$$f_b(\langle \sigma_{r1}^1 \rangle) = \int_{\sigma_{min}}^{\sigma_{max}} \frac{V}{V_0} \cdot \frac{1}{\sigma_0^m} \cdot \langle \sigma_{r1}^1 \rangle^m \cdot p(\sigma) d\sigma \quad (12)$$

with $p(\sigma)$ the probability density function of the inter-particle stress distribution, σ_{min} and σ_{max} the minimum and maximum stress value, respectively.

The rectangular and triangular stress distributions are supposed symmetric with respect to the average stress. They are thus uniquely defined by their mean and their standard deviation. We denote \bar{s} the standard deviation normalized by the mean longitudinal stress. Resolving Eq.12 for the two distributions yields:

$$f_b(\langle \sigma_{r1}^1 \rangle) = \frac{V}{V_0} \cdot \left(\frac{\langle \sigma_{r1}^1 \rangle}{\sigma_0} \right)^m \cdot g(\bar{s}, m) \quad (13)$$

where $g(\bar{s}, m)$ is a function of the standard deviation, the mean longitudinal stress in the particles and the Weibull modulus. Explicit expressions for both the rectangular and the triangular distribution are given in Eqs. 14 and 15, respectively.

$$g_u(\bar{s}, m) = \frac{(1 + \bar{s}\sqrt{3})^{m+1} - (1 - \bar{s}\sqrt{3})^{m+1}}{\sqrt{12} \cdot (m+1) \cdot \bar{s}} \quad (14)$$

$$g_t(\bar{s}, m) = \frac{(1 + \bar{s}\sqrt{6})^{m+2} + (1 - \bar{s}\sqrt{6})^{m+2} - 2}{6 \cdot \bar{s}^2 \cdot (m+1) \cdot (m+2)} \quad (15)$$

Finite element simulations suggest that the standard deviation of the stress in the particles remains small as long as the matrix deforms in the elastic regime, and then increases with increasing matrix plasticity. A typical value for the plastic regime is $\bar{s} = 0.3$ for a composite with 0.2 volume fraction of spherical reinforcement, [4].

Replacing Eq. 2 by Eq. 13 and following the procedure presented in Section 3.1, the stress-strain curve of a (damaging) composite having a non-uniform particle stress can then also be calculated, as well as the onset of tensile instability.

In these modelling approaches (without or with a particle stress distribution), it is implicitly assumed that the load shed by a fractured particle is redistributed uniformly over the remaining material; it is in this sense that this calculation corresponds to the global load sharing (GLS) mode of failure of a continuous fibre reinforced composite under longitudinal loading. We now turn to the opposite extreme, of local load sharing.

3.3 Catastrophic Failure

In contrast to the above, we can also consider the opposite case, i.e., assume that the load shed by a fractured particle is entirely redistributed over its immediate neighbouring particles only; this corresponds to (fully) local load sharing, LLS. The implication is that fracture of a particle causes a stress concentration in its immediate neighbours, raising in turn their probability of fracture. This may induce a cascade of particle fractures and thus cause the catastrophic failure of the composite.

Batdorf [37] proposed an elegant treatment of the problem for fibre-reinforced composites, by consideration of the formation probability of a cluster of i broken fibres (named an “i-plet”) and the stress redistribution around it. This model can be transposed to describe the fracture of a particulate composite.

We describe particle failure statistics using the simplified, low f_b , Weibull expression given in Eq. 11. If the composite contains N particles, when the stress on the particles reaches $\langle \sigma_{r1}^1 \rangle$ the number of single (uncorrelated) particle breaks Q_i (“singlets”) becomes:

$$Q_i = N \cdot \frac{V}{V_0} \cdot \left(\frac{\langle \sigma_{r1}^1 \rangle}{\sigma_0} \right)^m \quad (16)$$

The creation of a singlet generates a stress increase in neighbouring particles, and this may cause one of them to fracture as well, i.e., induce the formation of a doublet. This may in turn induce the formation of multiplets.

We assume that only direct neighbours that lie in the plane normal to the tensile direction containing the i-plet are overloaded. These particles thus carry a locally increased stress:

$$\sigma_{r1}^1 = c_i \cdot \langle \sigma_{r1}^1 \rangle \quad (17)$$

The stress concentration factor c_i can be calculated under the assumption that the fraction of

broken particles remains low, i.e., we assume that both the average stress borne by the matrix and the fraction of intact particles remain essentially unchanged.

Since the difference between the stress carried by an intact particle and that carried by a broken particle (equal to the matrix stress as assumed here [32]) is then redistributed (only) onto the n_i neighbours of the i-plet, we obtain for the stress in neighbouring overloaded particles, σ_{r1}^1 :

$$\sigma_{r1}^1 = \left(\langle \sigma_{r1}^1 \rangle - \langle \sigma_m^1 \rangle \right) \cdot \frac{i}{n_i} + \langle \sigma_{r1}^1 \rangle \quad (18)$$

The VE-MT model and Eq. 5 then lead to a simple expression for c_i :

$$c_i = 1 + \frac{2}{4 + V_r} \cdot \frac{i}{n_i} \quad (19)$$

The number of close neighbours of an i-plet, assuming a hexagonal array of particles in the plane normal to the loading axis, can be found in [38].

The probability that an i-plet becomes an (i+1)-plet is:

$$P_{i \rightarrow i+1} = \frac{n_i \cdot V}{V_0} \cdot \left(\frac{c_i \cdot \langle \sigma_{r1}^1 \rangle}{\sigma_0} \right)^m \quad (20)$$

such that the number of (i+1)-plets is:

$$Q_{i+1} = Q_i \cdot P_{i \rightarrow i+1} \quad (21)$$

A general expression then results from the recursion equation Eq. 21:

$$Q_i = N \cdot \left(\frac{\langle \sigma_{r1}^1 \rangle}{\sigma_0} \right)^{im} \prod_{j=1}^{i-1} c_j^m \cdot n_j \quad (22)$$

with Eq. 22 one can draw curves of $Q_i = f(\langle \sigma_{r1}^1 \rangle)$ on a double logarithmic plot, Fig. 3. If $Q_{i+1} > Q_i$, the (i+1)-plet cannot exist, since an (i+1)-plet arises from an i-plet (this is an artefact of using Eq. 11); all Q_{i+1} curves are thus interrupted where they meet the Q_i curve. The end result is an envelope of curves corresponding to unstable i-plets, i.e., ones that immediately become (i+1)-plets. The failure stress of the composite then corresponds to the lowest stress at which an unstable i-plet is created with near certainty, i.e., where this envelope crosses the axis $Q_i = 1$, Fig. 3.

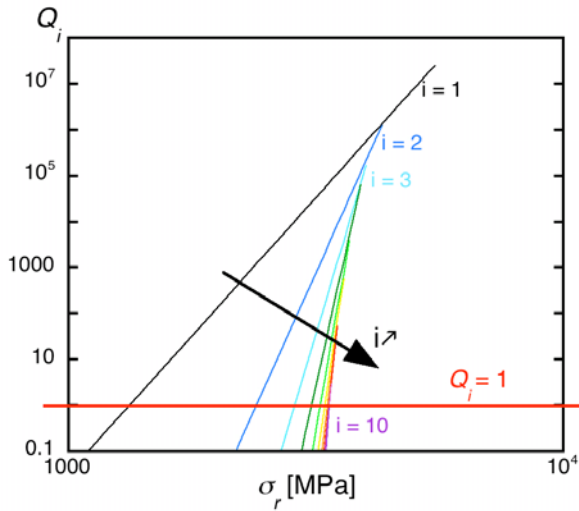


Fig. 3. Plot of $\ln(Q_i)$ as a function of $\ln(\sigma_r)$. With data for Nextel™ fibres (Table 1) fracture occurs for $i = 10$.

Therefore, this model provides the average stress acting on intact particles that will generate an unstable cluster of broken particles, and also the size of this unstable cluster. Typically, in this fracture mode the build-up of internal damage ahead of final fracture is relatively small. Hence the strength of the composite can be calculated using Eq. 5.

We note that, under the assumptions made here, the composite LLS fracture stress is independent of the matrix properties.

For this local load sharing approach, the stress acting on the reinforcements is not assumed to follow a distribution, contrary to what has been considered for the GLS case. This is mainly because of the difficulty involved in incorporating a stress distribution into the previous calculation; however, one might expect the influence of particle-to-particle stress fluctuations to be lower in fracture by local load sharing. Indeed, fluctuations in particle stress result from local interactions, between the particles and between particle and matrix. Therefore, over a group of, say, ten neighbouring particles (Fig. 3), one would expect the average particle stress to be relatively near the average particle stress over the entire composite, or in other words neighbours of overstressed particles to be understressed and vice-versa. This might smoothen stress distribution heterogeneity effects.

4 Results and Discussion

Predicted composite strength data are given in Table 2, together with the predicted failure mode. As

can be readily seen, composites made with particles having the same statistical strength as current engineering ceramic fibres are predicted to break essentially with no damage, therefore featuring a tensile ductility almost identical to that of the matrix from which they are made (with no particle failure, this comes out naturally from the model since the composite then features the same stress exponent as its matrix). Clearly, this is at odds with experimental data, including data collected with vapour-grown alumina particles of far higher perfection than comminuted particles generally used to produce particle reinforced aluminium composites.

Table 2. Predicted composite strength data generated under the assumption of a homogeneous particle stress.

Particle properties	Catastrophic failure		Failure by tensile instability			Failure mode
	Σ_c [MPa]	f_b [%]	Σ_c [MPa]	$\epsilon_{c,pl}$ [-]	f_b [%]	
Nextel™ [24]	2620	0.36	725	0.17	$7 \cdot 10^{-8}$	tensile instability
Altex™ [25]	2585	1.6	725	0.17	$9 \cdot 10^{-3}$	tensile instability

Incorporating a particle stress distribution into the model (Eqs. 13 to 15, with $\bar{s} = 0.3$) is not sufficient to induce a realistic amount of particle fracture in an Al-4.5%Cu matrix if the particles have the same properties as Nextel™ or Altex™ fibres. A value of \bar{s} as high as 2.5 is necessary to break 5% particles with Nextel™ properties when these are loaded with a triangular stress distribution. For particles with Altex™ properties an even larger standard deviation would be needed in order to induce a substantial amount of particle fractures. No realistic distribution of stresses can thus explain why modelled composites are so strong compared to real existing ones.

The reason must therefore be that real particles are in fact far less strong than current engineering ceramic fibres. This is obviously true for comminuted ceramic particles, well known to contain internal defects in the form of pores or cracks, as well as sites of stress concentration given their angular shape. In an elegant study by Qin et al.[39], such particles were blunted by high-speed-air, and this indeed resulted in improved composite properties, by removing sites of stress concentration and thus decreasing the possibility of particle corner fracturing. More surprisingly, Sumitomo's Sumicorundum™ particles, although

much better than comminuted particles, also underperform what would be found were ceramic fibre properties matched. Seemingly there is at present ample room for the improvement of ceramic particles used to reinforce metals.

Particle Weibull parameters yielding more realistic composite properties, namely $m = 10$ and $\sigma_0 = 1200$ MPa, are used in Fig. 4 where only failure by tensile instability is considered. The modelled composite features 5% of broken particles at failure with a homogeneous particle stress. Introducing a particle stress distribution ($\bar{s} = 0.3$) increases the fraction of broken particles to 15 or 16% for a rectangular or a triangular stress distribution, respectively. The fracture stress is thus lowered from 684 MPa to 577 MPa and the fracture strain from 13.6 to 7% by the introduction of a triangular particle stress distribution instead of a homogeneous stress. Clearly particle stress inhomogeneity is an important factor in damage and tensile failure of particle reinforced metals.

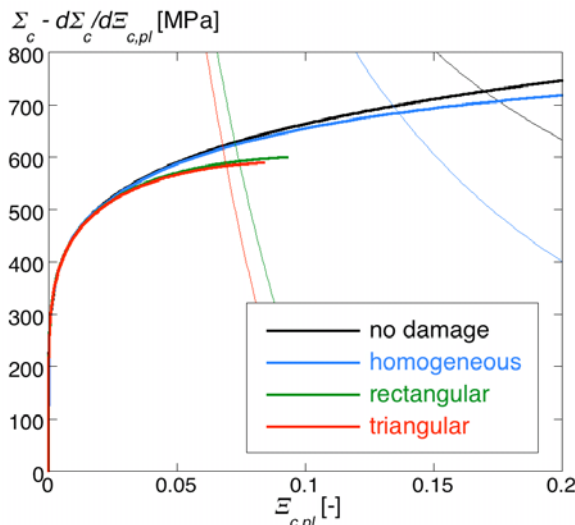


Fig. 4. Comparison of the influence of different particle stress distributions (homogeneous, rectangular and triangular) on failure by tensile instability. Al-4.5%Cu matrix reinforced with 50 vol.pct. particles ($m = 10$, $\sigma_0 = 1200$ MPa).

Still using these more realistic particle properties, we now examine the role of the matrix on the failure mode of the composite, Fig. 5 (a) and (b). An Al-2%Cu matrix ($c = 420$ MPa and $n = 0.17$) induces fracture by tensile instability, contrary to a (stronger) Al-4.5%Cu matrix, which induces catastrophic failure. Despite its many simplifications and the large room still left for its improvement, the present analysis thus mimics the experimental

finding that stronger matrices can yield more brittle composites by changing the failure mode from tensile instability to catastrophic failure.

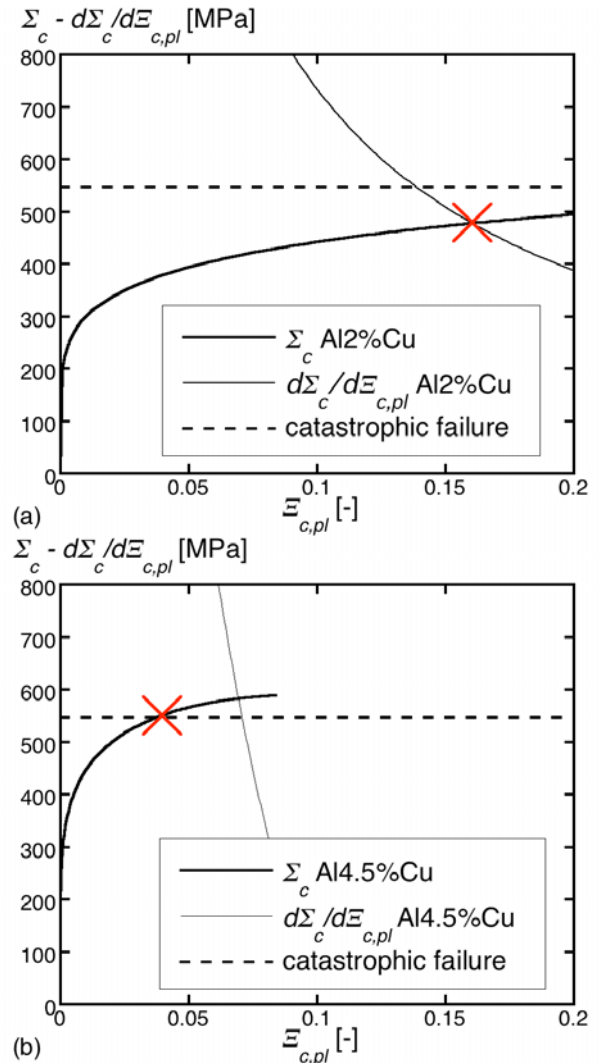


Fig. 5. Influence of the matrix material on the failure mode of a particle reinforced composite. (a) With an Al-2%Cu matrix failure occurs by tensile instability. (b) With an Al-4.5%Cu matrix failure is catastrophic.

5 Conclusions

The extension to ceramic particles of ceramic fibre processing technology, enabling the production of particles having Weibull parameters similar to those of today's ceramic fibres, could yield very attractive metal matrix composites. Indeed, we show here that if damage occurs only by particle fracture, such materials would match their matrix in terms of ductility—while being significantly stronger and stiffer. Matrix voiding, not considered in the present

analysis, will of course then play a strong role (rules to optimize the matrix in this regard are discussed in Ref. [19]) but with particle fracture absent, strong improvements in composite properties still remain likely. From an engineering standpoint, therefore, we conclude that there is an exciting window of opportunity in the processing of strong ceramic particles for the reinforcement of metals.

The simplified models used here account satisfactorily for the two observed failure modes of highly loaded particle reinforced metal matrix composites. In particular the observed transition, with increasing matrix hardness, from fracture by tensile instability to catastrophic failure is explained. The analysis has, however, wide room for improvement, in several regards. The most obvious improvement would be to use the complete (exponential) Weibull formulation, if only because observed fractions of broken particles in these composites are large. Another obvious improvement would be the development of more realistic stress concentration factors for particles neighbouring an i-plet; in this regard numerical 3D calculations of highly packed multi-particle cells would be very useful. Such simulations can, indeed, give directly the patterns of stress redistribution surrounding a broken particle. These, in turn, could be used in the present local load sharing fracture model in the form of improved c_i factors having higher precision than those estimated here by direct load shedding from broken particles to a fixed i -dependent number of neighbouring particles. And finally, methods for the direct experimental assessment of intrinsic particle properties would be both helpful and, *per se*, very interesting.

6 Acknowledgements

This research was supported by the Swiss National Science Foundation, Project No. 200020-107556.

7 References

- [1] Ponte Castañeda P. and Suquet P. "Nonlinear composites". *Advances in Applied Mechanics*, van der Giessen E. and Wu T. Y., Editors, Vol. 34, pp 171-302, Academic Press, 1998.
- [2] Llorca J. "Void formation in metal matrix composites". *Comprehensive Composite Materials*, Kelly A. and Zweben C., Editors, Vol. 3.04, pp 91-115, Pergamon, 2000.
- [3] Pierard O., Llorca J., Segurado J. and Doghri I. "Micromechanics of particle-reinforced elasto-viscoplastic composites: Finite element simulations versus affine homogenization". *International Journal of Plasticity*, Vol. 23, No. 6, pp 1041-1060, 2007.
- [4] Han W., Eckschlager A. and Böhm H. J. "The effects of three-dimensional multi-particle arrangements on the mechanical behavior and damage initiation of particle-reinforced MMCs". *Composites Science and Technology*, Vol. 61, No. 11, pp 1581-1590, 2001.
- [5] Chawla N. and Chawla K. K. "Metal matrix composites". Springer, 2006.
- [6] Clyne T. W. and Whiters P. J. "An introduction to metal matrix composites". Cambridge University Press, 1993.
- [7] Mochida T., Taya M. and Obata M. "Effect of damaged particles on the stiffness of a particle/metal matrix composite". *JSME International Journal*, Vol. 34, No. 2, pp 187-193, 1991.
- [8] Zhao Y. H. and Weng G. J. "Plasticity of a two-phase composite with partially debonded inclusions". *International Journal of Plasticity*, Vol. 12, No. 6, pp 781-804, 1996.
- [9] Segurado J. and Llorca J. "A new three-dimensional interface finite element to simulate fracture in composites". *International Journal of Solids and Structures*, Vol. 41, No. 11-12, pp 2977-2993, 2004.
- [10] Llorca J. and Segurado, J. "Three-dimensional multiparticle cell simulations of deformation and damage in sphere-reinforced composites". *Materials Science and Engineering A*, Vol. 365, No. 1-2, pp 267-274, 2004.
- [11] Eckschlager A., Han W. and Böhm H. J. "A unit cell model for brittle fracture of particles embedded in a ductile matrix". *Computational Materials Science*, Vol. 25, No. 1-2, pp 85-91, 2002.
- [12] Boyd J. D. and Lloyd D. J. "Clustering in particulate MMCs". *Comprehensive Composite Materials*, Kelly A. and Zweben C., Editors, Vol. 3.06, pp 139-149, Pergamon, 2000.
- [13] Mishnaevsky L. L. "Three-dimensional numerical testing of microstructures of particle reinforced composites". *Acta Materialia*, Vol. 52, No. 14, pp 4177-4188, 2004.
- [14] Mishnaevsky L., Derrien K. and Baptiste D. "Effect of microstructure of particle reinforced composites on the damage evolution: Probabilistic and numerical analysis". *Composites Science and Technology*, Vol. 64, No. 12, pp 1805-1818, 2004.
- [15] Kouzeli M., Weber L., San Marchi C. and Mortensen A. "Influence of damage on the tensile behaviour of pure aluminium reinforced with ≥ 40 vol. pct alumina particles". *Acta Materialia*, Vol. 49, No. 18, pp 3699-3709, 2001.
- [16] Kouzeli M. and Mortensen A. "Size dependent strengthening in particle reinforced aluminium". *Acta Materialia*, Vol. 50, No. 1, pp 39-51, 2002.

- [17] Miserez A., Stuecklin S. and Mortensen A. "Influence of heat treatment and particle shape on mechanical properties of infiltrated Al₂O₃ particle reinforced Al-2wt-%Cu". *Materials Science and Technology*, Vol. 18, pp 1461-1470, 2002.
- [18] Miserez A. and Mortensen A. "Fracture of aluminium reinforced with densely packed ceramic particles: Influence of matrix hardening". *Acta Materialia*, Vol. 52, No. 18, pp 5331-5345, 2004.
- [19] Miserez A., Mueller R. and Mortensen A. "Increasing the strength/toughness combination of high volume fraction particulate metal matrix composites using an Al-Ag matrix alloy". *Advanced Engineering Materials*, Vol. 8, No. 1-2, pp 56-62, 2006.
- [20] Curtin W. A. "Stochastic damage evolution and failure in fiber-reinforced composites". *Advances in Applied Mechanics*, van der Giessen E. and Wu T. Y., Editors, Vol. 36, pp 163-253, Academic Press, 1999.
- [21] Phoenix S. L. and Beyerlein I. J. "Statistical strength theory for fibrous composite materials" *Comprehensive Composite Materials*, Kelly A. and Zweben C., Editors, Vol. 1.19, pp 559-639, Pergamon, 2000.
- [22] Argon A. S. "Fracture: Strength and toughness mechanisms". *Comprehensive Composite Materials*, Kelly A. and Zweben C., Editors, Vol. 1.24, pp 763-802, Pergamon, 2000.
- [23] Mueller R. and Mortensen A. "Simplified prediction of the monotonic uniaxial stress-strain curve of non-linear particulate composites". *Acta Materialia*, Vol. 54, No. 8, pp 2145-2155, 2006.
- [24] Wilson D. M. "Statistical tensile strength of Nextel™ 610 and Nextel™ 720 fibres". *Journal of Materials Science*, Vol. 21, pp 2535-2542, 1997.
- [25] Bushby R. S. "Evaluation of continuous alumina fibre reinforced composites based upon pure aluminium". *Material Science and Technology*, Vol. 14, pp 877-886, 1998.
- [26] Chi Z., Chou T. W. and Shen G. "Determination of single fibre strength distribution from fibre bundle testings". *Journal of Materials Science*, Vol. 19, pp 3319-3324, 1984.
- [27] Matthewson M. J., Kurkjian C. R. and Gulati S. T. "Strength measurement of optical fibers by bending". *Journal of the American Ceramic Society*, Vol. 69, No. 11, pp 815-821, 1986.
- [28] Weber L., Kouzeli M., San Marchi C. and Mortensen A. "On the use of Considere's criterion in tensile testing of materials which accumulate internal damage". *Scripta Materialia*, Vol. 41, No. 5, pp 549-551, 1999.
- [29] Derrien K., Fitoussi J., Guo G. and Baptiste D. "Prediction of the effective damage properties and failure properties of nonlinear anisotropic discontinuous reinforced composites". *Computer Methods in Applied Mechanics and Engineering*, Vol. 185, No. 2-4, pp 93-107, 2000.
- [30] Hu G. K., Guo G. and Baptiste D. "A micromechanical model of influence of particle fracture and particle cluster on mechanical properties of metal matrix composites". *Computational Materials Science*, Vol. 9, No. 3-4, pp 420-430, 1998.
- [31] Mueller R. "Tensile behavior of aluminium alloys reinforced with ceramic particles". *Doctoral Thesis*, Ecole Polytechnique Fédérale de Lausanne (EPFL), Lausanne, Switzerland, 2007.
- [32] Mueller R., Rossoll A., Weber L. and Mortensen A. "Influence of damage on the uniaxial flow stress of ceramic particle reinforced metals. Part 1: Analysis". *In preparation*, 2007.
- [33] Mueller R., Kouzeli M., Rossoll A., Weber L. and Mortensen, A. "Influence of damage on the uniaxial flow stress of ceramic particle reinforced metals. Part 3: Scale dependence of plastic flow". *In preparation*, 2007.
- [34] Segurado J. and Llorca J. "Computational micromechanics of composites: The effect of particle spatial distribution". *Mechanics of Materials*, Vol. 38, No. 8-10, pp 873-883, 2006.
- [35] Böhm H. J. and Han W. "Comparisons between three-dimensional and two-dimensional multi-particle unit cell models for particle reinforced metal matrix composites". *Modelling and Simulation in Materials Science and Engineering*, Vol. 9, No. 2, pp 47-65, 2001.
- [36] Shen H. and Lissenden C. J. "Stress and strain localization three-dimensional modeling for particle-reinforced metal matrix composites". *Metallurgical and Materials Transactions A-Physical Metallurgy and Materials Science*, Vol. 36A, No. 7, pp 1653-1660, 2005.
- [37] Batdorf S. B. "Tensile strength of unidirectionally reinforced composites - I". *Journal of Reinforced Plastics and Composites*, Vol. 1, pp 153-164, 1982.
- [38] Moser B. "Deformation and fracture of continuous alumina fibre reinforced aluminium composites". *Doctoral Thesis*, Ecole Polytechnique Fédérale de Lausanne (EPFL), Lausanne, Switzerland, 2002.
- [39] Qin S., Chen C., Zhang G., Wang W. and Wang Z. "The effect of particle shape on ductility of SiCp reinforced 6061 Al matrix composites". *Materials Science and Engineering A*, Vol. 272, No. 2, pp 363-370, 1999.